THE JOURNAL OF PHYSICAL CHEMISTRY B
A JOURNAL OF THE AMERICAN CHEMICAL SOCIETY

pubs.acs.org/JPCB

Article

Molecular Weight Dependence of Surface Tension of Poly(ethylene oxide) Solution

Jianwei Zhang, Lu Qian, Jiajia Zhou,* and Guangzhao Zhang*

Cite This: J. Phys. Chem. B 2023, 127, 6743−6750

Read Online

ACCESS | Metrics & More | Article Recommendations | Supporting Information

ABSTRACT: Surface tension plays a critical role in a wide range of fields such as adhesion, wetting, and capillarity. Herein, we combine experiments and molecular dynamics (MD) simulations to study the surface tension (γ) of poly(ethylene oxide) (PEO) solution as a function of its molecular weight (M). In experiments, we reveal that γ is scaled to M with $|\gamma - \gamma_\infty| \propto M^\alpha$ up to a critical molecular weight (M^*). Simulation with a coarse-grained polymer solution model shows that α decreases as the solvent quality becomes worse. The combination of the experiments and simulations reveal that α is slightly affected by PEO concentration. On the other hand, M^* decreases as the solvent quality decreases or as the polymer concentration increases. Our study demonstrates that the surface tension of the polymer solution is determined by the adsorption of the polymer at the air−solution surface.

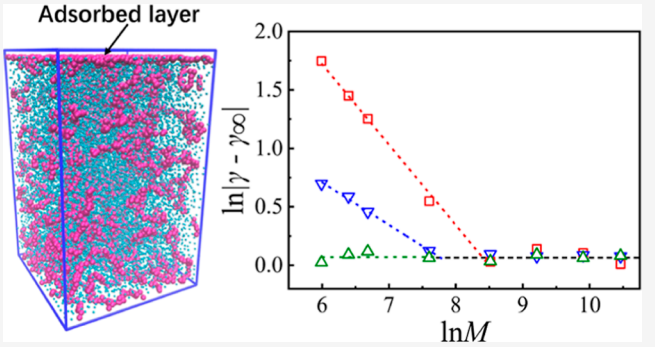

INTRODUCTION

Surface tension of polymeric liquids (melt or solution) has received continuing interest because it plays an important role in coatings, adhesives, polymer blends, and polymer composites and in determining the properties of the adhesion, capillarity, wettability, and compatibility.[1] In addition, molecular dependence of polymer basic properties (e.g., viscosity, interfacial friction, phase separation, thermoelectric property, etc.) has been a significant subject for decades due to its advantage to meet the application requirements in different situations.[2−6] For polymeric liquids, Legrand and Gaines[7] presented the following equation to describe the relation between the surface tension γ and polymer molecular weight M

$$\gamma = \gamma_\infty - KM^\alpha \quad (1)$$

where $\gamma\infty$ is the surface tension at infinite molecular weight and K is a constant depending on the nature of polymer. This equation was validated in many polymer melt systems.[8−13] The exponent α is determined to be −1 for polymers of high molecular weight and −2/3 for polymers of low molecular weight. However, it remains difficult to identify the boundary between these two scenarios.[14]

In the past decades, the factors influencing the surface tension in polymer melts have been systematically investigated. It shows that the chain ends and the density variation play critical roles. For the former, de Gennes[15] derived eq 1 using the scaling argument and obtained the exponent $\alpha = -1/2$. Aubouy et al.[16] described the interface properties of the polymer melt based on the loop density profile and proposed relation $\Delta\gamma \propto \ln (M_n/M_n^*)/M_n^{1/2}$. However, their result was questioned[17,18] and probably more experimental data are needed.[19] Molecular dynamics simulations were also used to verify the role of the terminal segments.[20] On the other hand, based on the early work of Cahn and Hilliard,[21] the variation of the melt density with molecular weight was considered as the primary contribution to the molecular weight dependence of surface tension.[22] This was supported by studies that separated the contribution of the chain-end segregation and the density variation.[23] The comparison of previous works on the scaling relation between γ and M is shown Table S1.

The scaling relation between γ and M of polymer solution is also of profound significance in its wetting process. For example, many nanofabrications such as template-assisted nanofabrication needs us to accurately predict the wetting process between polymer solution and anodized aluminum oxide templates, which is determined by both polymer type and surface tension of solution.[24] Capillary filling of polymer liquid in the nanoscale also plays a critical role in many techniques such as modern lab-on-chip applications, which is instructed by the Lucas−Washburn theory where molecular weight dependence of surface tension is indispensable.[25−27]

Received: March 14, 2023
Revised: July 11, 2023
Published: July 24, 2023

https://doi.org/10.1021/acs.jpcb.3c01719
J. Phys. Chem. B 2023, 127, 6743−6750

Furthermore, the most common technique to make polymer films or substrates with nano-pattern is based on polymer solution, even involves the exchange of solutes and polymer blends.[28−31] Therefore, it is necessary to understand the surface tension of the polymer solution for better design of more sophisticated products. However, for polymer solution composed of polymer solute and small molecule solvent, the situation is more complex than the polymer melt. According to Flory−Huggins theory,[32] the solution concentration, polymer molecular weight, solvent, and polymer−solvent interactions would all contribute to the free energy of the solution. Therefore, all the above factors can influence the surface tension of the polymer solution. The effect of polymer concentration has been studied in the past.[33−40] Considering that it generally interplays with molecular weight dependence, the exact role played by either of them remains unclear.[16] Actually, the surface behavior of polymer solution is associated with the adsorption or packing of polymer chains on the air−solution surface.[41−49] As the free energy of pure solvent and polymer is not equal, the surface tension of polymer solution should depend on their volume ratio. Thus, adsorption of the polymer should profoundly influence the surface tension of polymer solution. We deem it is also the main mechanism behind the molecular weight dependence of surface tension in the case of polymer solutions.

In the present work, we have investigated the surface tension γ of poly(ethylene oxide) (PEO) solution as a function of its molecular weight M by a combination of experiment and simulation. Our study reveals that $(\gamma - \gamma_\infty) \propto M^\alpha$ when $M < M^*$, but γ is then independent of M when $M > M^*$, where M^* is the critical molecular weight. We also demonstrate that the dominant factor in this relation is the amount of adsorbed polymer chains at the air−solution surface by correlating the surface tension and polymer adsorption.

METHODS

Experimental Materials. All PEO samples with a small polydispersity ($M_w/M_n < 1.14$) were purchased from Innochem and Sigma-Aldrich. The samples used have number average molecular weights M_n of 4.0×10^2, 6.0×10^2, 8.0×10^2, 2.0×10^3, 5.0×10^3, 1.0×10^4, 2.0×10^4, 3.5×10^4, 3.0×10^5, and 6.0×10^5 g/mol, respectively. To prepare polymer solutions, Milli-Q water, ethyl alcohol, and chloroform (AR) were used as the solvent. To test the effect of solution concentration, aqueous solution of PEO with seven different volume fractions $\Phi_{PEO} = \frac{V_{PEO}}{V_{PEO} + V_{solvent}} = 7.900 \times 10^{-4}$, 2.400×10^{-3}, 7.900×10^{-3}, 1.185×10^{-2}, 1.580×10^{-2}, 1.975×10^{-2}, and 2.400×10^{-2} were prepared. More precisely, using volume fractions as solution concentration here means when we change the molecular weight of PEO at a certain concentration, the number and length of PEO chains change but the number of EO units remains constant. This setting is because the PEO volume fraction of the surface, or the number of EO units at the surface, determines the value of surface tension. To test the effect of solvent, PEO in chloroform when $\Phi_{PEO} = 7.900 \times 10^{-4}$, and PEO in the water−ethanol mixture with 0, 4, and 35 wt % ethanol when $\Phi_{PEO} = 7.900 \times 10^{-3}$ were prepared.

Surface Tension Measurement. We used the pendent drop method to measure the surface tension of the polymer solution by an automatic surface tension detector (Biolin, Attention), and the details of the principle have been given elsewhere.[50] Experiments were performed at 25 °C. The volume of single droplet is 7 μL each time and suspended at the bottom of the pipette. Recording and analyzing time were set at every 0.25 s for a total of 10 s for every drop. Each sample was tested 20 times to take an average surface tension value to improve the measurement precision. All tests were run after enough time to make adsorption of PEO reach dynamical equilibrium, so that the impact of diffusion of PEO chains around the surface on the value of surface tension can be ignored.

Simulation Details. We performed Langevin simulations to measure the surface tension of the polymer solution. Solvent molecules were modeled as spherical beads and linear polymer chains were modeled by the beads connected by harmonic springs. The unbonded interactions between all beads were modeled by the truncated-shifted Lennard-Jones (LJ) potential.

$$U_{LJ}(r) = \begin{cases} 4\varepsilon_{LJ}\left[\left(\frac{\sigma}{r_{ij}}\right)^{12} - \left(\frac{\sigma}{r_{ij}}\right)^{6} - \left(\frac{\sigma}{r_{cut}}\right)^{12} + \left(\frac{\sigma}{r_{cut}}\right)^{6}\right] & r_{ij} \le r_{cut} \\ 0 & r_{ij} > r_{cut} \end{cases} \quad (2)$$

where r_{ij} is the distance between the ith and jth beads, and σ is the bead diameter. Conventionally, reduced units are adopted in the rest of the paper. The LJ interaction parameter ε_{LJ} was equal to $1.0k_BT$ for interactions between beads. The cutoff distance r_{cut} between the same beads was set to $\sqrt[6]{2}\sigma$ using the repulsive part of the LJ potential to mimic the excluded-volume effect. To model different solvent conditions, we set $r_{cut} = 1.3\sigma$, 1.5σ, and 1.7σ between the polymer and the solvent. The bonded potential is

$$U(r) = k(r - r_0)^2 \quad (3)$$

where r is the distance between two connected beads, k and r_0 were set to $150k_BT/\sigma^2$ and 0.65σ.

The simulation box has a size of $L_x \times L_y \times L_z$ with periodic boundary conditions (PBC) along the direction of x, y-axes and we set $L_x = L_y = 25\sigma$ and $L_z = 40\sigma$. To present the interface that has positive adsorption to the solute, the planar structureless wall was set at $z = 0$ and $z = 40$ with $\varepsilon_{LJ} = 1.0k_BT$ and $r_{cut} = \sqrt[6]{2}\sigma$ for solvent, $\varepsilon_{LJ} = 2.0k_BT$ and $r_{cut} = 2.5\sigma$ for polymer. The density of the solution was chosen as $\rho = 0.72\sigma^{-3}$.

The solvent quality is determined by the scaling relation between the mean square radius of gyration R_g and the degree of polymerization N ($R_g \propto N^\nu$) as shown in Figure S1. The calculation details of R_g is provided in the Supporting Information section. The result shows that all our simulations are performed with a good solvent since $\nu \approx 0.63$ is close to the theoretical value 0.6. Furthermore, the larger r_{cut} implies the larger attractive interaction between the polymer and solvent. As absolute value of R_g increases with r_{cut}, we determine that the solvent with $r_{cut} = 1.7\sigma$ has a better solvent quality than the solvent with $r_{cut} = 1.3\sigma$ in our model.

The surface tension of the system is calculated by integrating the asymmetry of the pressure tensor according to Irving−Kirkwood's expression[51]

$$\gamma = \frac{1}{2}\int_0^{L_z} [P_N(z) - P_T(z)]\, dz \quad (4)$$

where $P_N(z)$ and $P_T(z)$ are the pressure in the normal and the lateral direction to the walls. According to the diagonal

https://doi.org/10.1021/acs.jpcb.3c01719
J. Phys. Chem. B 2023, 127, 6743−6750

elements of the pressure tensor, they can be given as $P_N(z) = P_{zz}(z)$, $P_T(z) = \frac{(P_{xx}(z) + P_{yy}(z))}{2}$. Additionally, since the interaction parameters between solvent beads remain unchanged for all the simulations, γ of the pure solvent should remain constant. Furthermore, the finite-size effect in our simulation is checked. On the one hand, we perform a model similar with the work by Meddah et al.,[20] where they have shown the lack of finite-size effects on the pressure in the direction with PBC. Along the direction of z-axis, they find the change in box size decrease the pressure, but the effect becomes weak gradually, and eventually ignorable when $L_z \geq 40\sigma$. On the other hand, in order to make a further check, we perform the case of longest chain system of $N = 200$ with same parameters in a larger box of $L_x = L_y = 40\sigma$ and $L_z = 60\sigma$. As shown in Figure S2, there is only slight change in the pressure of system when the box is larger, which means the finite-size effect has no significant influence.

The MD integration time step is $\delta t = 0.005\tau$ ($\tau = \sqrt{m\sigma^2/\varepsilon} = 1$ the MD time unit). System trajectories of polymers with length $20 \leq N \leq 200$ were computed with the velocity-Verlet algorithm,[52] applying a Langevin thermostat within the LAMMPS[53] simulation package.

RESULTS AND DISCUSSION

The surface tension γ of PEO aqueous solutions as a function of PEO molecular weight M is shown in Figure 1a. As the water−air interface is an attractive surface for PEO, the surface tension decreases with the increase in solution concentration. Figure 1b shows the result of taking the logarithm of data in Figure 1a. Clearly, the relation between surface tension and the molecular weight is consistent with eq 1 when the molecular weight is lower than a critical molecular weight M^*. The exponents α determined by linearly fitting are shown in Figure 1c and the value of α is around −0.7. This illustrates that the scaling relation between $\gamma - \gamma_\infty$ and M still persists in polymer solutions with an extra condition $M < M^*$, where $\gamma\infty$ refers to the surface tension of polymer solution with molecular weight $M > M^*$. When $M > M^*$, the surface tension becomes independent of the molecular weight. As shown in Figure 1d, M^* is about equal to 9.9×10^3, 6.3×10^3, 4.3×10^3, 3.75×10^3, 4.45×10^3, 4.8×10^3, and 2.7×10^3 g/mol when $\Phi_{PEO} = 7.900 \times 10^{-4}$, 2.400×10^{-3}, 7.900×10^{-3}, 1.185×10^{-2}, 1.580×10^{-2}, 1.975×10^{-2}, and 2.400×10^{-2} respectively. Generally, M^* decreases as PEO volume fraction increases. It is known that such a M^* is absent in the case of polymer melts, namely, that $\ln|\gamma - \gamma_\infty|$ of polymer melt is linearly related to $\ln M$ holds in the full range of molecular weight. Clearly, the polymer solution is quite different from the polymer melt in the mechanism.

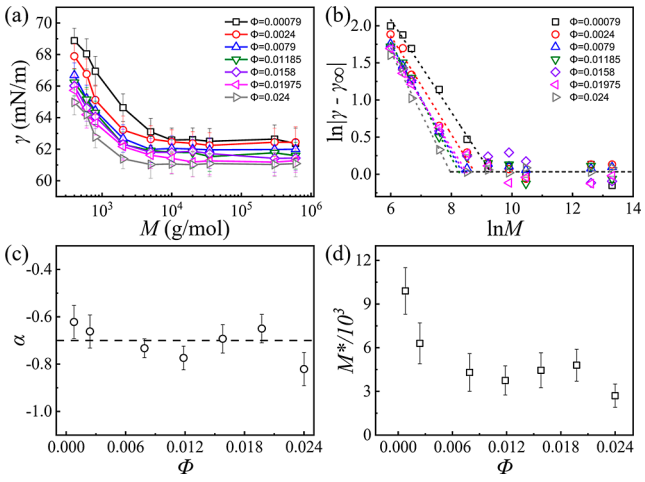

Figure 1. (a) Relation between surface tension γ and molecular weight M of PEO aqueous solutions at different volume fractions Φ. (b) The logarithm of the data of $\gamma - \gamma_\infty$ and M. (c) The exponent α of eq 1 collected by linearly fitting of the data in (b) (the slope of the left portion of figure). (d) The relation between critical molecular weight M^* and volume fractions Φ in above PEO aqueous solutions.

In polymer melts, there is no competition between solvent and solute molecules, so that the surface properties are determined by polymer chains only. The dominant factor influencing the surface tension is the variation in density[23] due to the change of molecular weight. In the case of PEO solutions, some PEO chains and different solvent molecules are adsorbed on the air−solvent surface, which determine the surface tension. Many studies[45−47,54] have shown an aggregation of PEO chains at the air−water surface so that γ would decrease as the amount of PEO at the surface increases. For the effect of molecular weight, Gilanyi et al.[44] demonstrated that longer PEO chains are more readily adsorbed at the surface by estimating the standard free energy of PEO adsorption. This is because the larger driving force, mainly contributed by the enthalpy, is exerted on long chains. This is understandable. Previous studies[55,56] revel PEO chains lie down at the surface with a locally serrated but overall irregular configuration. It is determined by the unfavorable interaction between hydrophilic end groups (−OH) and hydrophobic segments ($-CH_2-$) of the polyether. For the same concentration, the number of the hydrophilic end groups (−OH) decreases as molecular weight increases, so a longer chain becomes more hydrophobic. When the molecular weight reaches a critical value M^*, the amount of end groups relative to the hydrophobic methylene moieties is so small that their effect can be neglected, and the adsorption is independent of the molecular weight or chain length.

The adsorption isotherms of different molecular weight PEO chains are then calculated from the data of γ by means of the Gibbs equation

$$\Gamma = -\frac{1}{RT}\left[\frac{\partial\gamma}{\partial \ln(ac)}\right]_{T,p} \quad (5)$$

where Γ is the adsorption amount of solute, γ is the surface tension of solution, a is the activity coefficient and c is the concentration of solution. The adsorption isotherms in Figure 2a shows the saturation adsorbed amount of PEO at each molecular weight and each volume fraction of solution. The cases of Γ at $\Phi_{PEO} = 7.900 \times 10^{-3}$, 1.580×10^{-2}, and 2.400×10^{-2} are extracted and plotted into Figure 2b as a function of PEO molecular weight. The results show that the saturation adsorbed amount of all kinds of molecular weight PEO increases with its volume fraction in solutions. The saturation adsorbed amount of PEO also increases with its molecular weight at all concentrations, but the growth is tapering off and the curves go flat finally, as shown in Figure 2b. This trend of Γ is roughly consistent with the change in γ because the amount of PEO adsorbed at the surface determine the value of surface tension. We provide a plausible microscopic scenario in Figure S3 that attempts to reconcile the experimental findings.

https://doi.org/10.1021/acs.jpcb.3c01719
J. Phys. Chem. B 2023, 127, 6743−6750

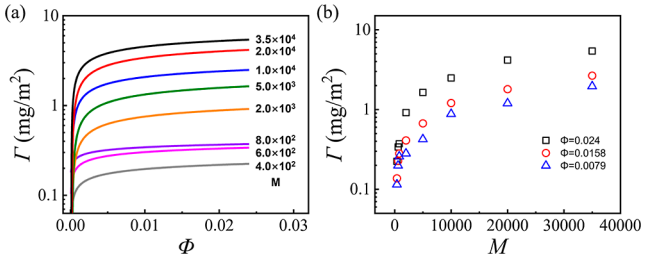

Figure 2. (a) Adsorption isotherms of different molecular weight PEO chains at the air−solution interface. (b) Saturation adsorbed amount of different molecular weight PEO chains at Φ_{PEO} = 7.900 × 10^{-3}, 1.580 × 10^{-2}, and 2.400 × 10^{-2}.

Combining the data of γ, the amount of PEO adsorbed at the surface can continue to increase at one certain concentration when $M < M^*$. The appearance of M^* in the relation between γ and M means that the amount of PEO adsorbed at the surface nearly keeps stable when $M \geq M^*$, so that the solution surface tension becomes independent on molecular weight. Furthermore, PEO chains with the same length gained larger driving force to be absorbed at the surface when PEO volume fraction is higher, as adsorption isotherms show. Thus, the fact that M^* decreases with PEO concentration indicates the solution with higher concentration could reach the stable adsorption amount even when chains are short. Figure S4 shows the surface tension data of PEO in DME at 20 °C, which further verifies $\gamma - \gamma_\infty$ is scaled to M even at different temperatures and different solvent conditions. The α and M^* in this situation equal to −0.705 and 5.0 × 10^3, respectively.

In order to make clear about the solvent effects on the scaling exponent α and the critical molecular weight M^*, we measured surface tension of PEO both in chloroform and water−ethanol mixture. As shown in Figure 3a,b, γ is independent of the PEO molecular weight in chloroform without M^* in the range we examined. The reason we believe is M^* goes below 400 g/mol (the minimum molecular weight of the sample) due to the change in solvent quality. As

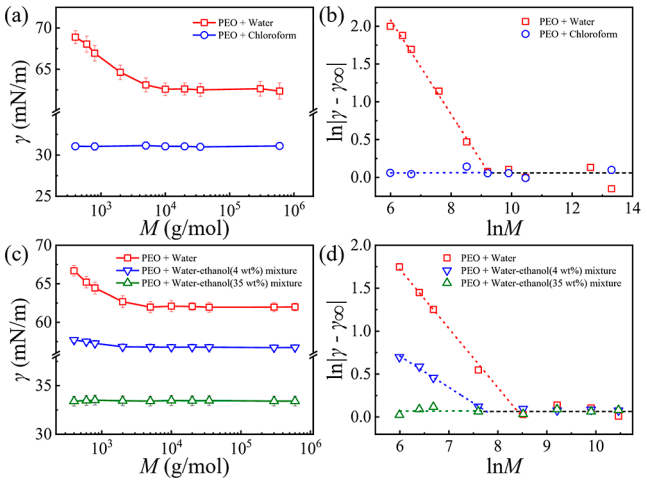

Figure 3. Effect of solvent on scale relation between γ and M: (a) PEO in water (red line) and in chloroform (blue line) at 25 °C and Φ_{PEO} = 7.900 × 10^{-4}. (b) The logarithm of the data of $\gamma - \gamma_\infty$ and M in (a). (c) PEO in water−ethanol mixture with 0 wt % ethanol (red line), 4 wt % ethanol (blue line), and 35 wt % ethanol (green line) at 25 °C, and Φ_{PEO} = 7.900 × 10^{-3}. (d) The logarithm of the data of $\gamma - \gamma_\infty$ and M in (c).

chloroform is a solvent worse than water for PEO,[57] the saturation of surface concentration happens at shorter chain length in the worse solvent. This can be attributed to that polymer chains have efficient dissolution in the good solvent and thus need to overcome a larger interaction with solvent to move to the surface.[58] In short, chains with the same length need a larger force to be driven to the surface in the good solvent. Thus, M^* decreases as the solvent gets worse.

To further clear about the solvent effect, we examined the surface tension of PEO in the water−ethanol mixture with different volume fractions of ethanol. In this system, the solvency can gradually become worse as the concentration of ethanol increases according to the second virial coefficient of solution, as shown in previous works.[59] The increasing R_g of PEO chains with the concentration of ethanol is another evidence.[60] Here, we evaluate the Flory−Huggins parameter χ between PEO and water−ethanol mixture with different concentrations of ethanol by $\chi_{PEO\text{-}mixture} = \varphi_{water}\chi_{PEO\text{-}water} + \varphi_{ethanol}\chi_{PEO\text{-}ethanol}$, where φ_{water} and $\varphi_{ethanol}$ are the volume fractions of water and ethanol of the water−ethanol mixture and $\chi_{PEO\text{-}water}$ and $\chi_{PEO\text{-}ethanol}$ are χ between PEO and pure water or pure ethanol. According to previous simulation methods and results,[61,62] $\chi_{PEO\text{-}water} \approx 0.3$ and $\chi_{PEO\text{-}ethanol} \approx 3.5$. Thus, $\chi_{PEO\text{-}mixture}$ = 0.3, 0.46, and 1.58 when the concentrations of ethanol are 0, 4, and 35 wt %, respectively.

As shown in Figure 3c,d, $\gamma - \gamma_\infty$ is also scaled to M though the index α increases as the solvent becomes worse, where α = −0.733, −0.365, and 0 corresponding to the case of 0, 4, and 35 wt % ethanol, respectively. On the other hand, M^* = 4.0 × 10^3, 2.0 × 10^3, and $M^* < 4.0 \times 10^2$ when the concentration of ethanol is 0, 4, and 35 wt %, respectively. Namely, M^* decreases as the solvent quality drops. Regarding the competition between PEO and mixture solvent at the surface, we assume that the composition of solvent molecules replaced by PEO at the surface is consistent with that in the bulk. So, that we could view the water and ethanol molecules as a whole according to their mass fraction. The competition between PEO and mixture at the surface is then same with the case of single kind of solvent. However, note that the fraction of ethanol in the water−ethanol mixture can change not only the solvent quality but also the surface tension of the solvent. The difference of the surface tensions between the pure solvent and pure solute should profoundly influence the adsorption. Considering that we cannot separate the effects in experiments, we performed molecular dynamics simulations to further clear about the role of the solvent.

The results of MD simulation reproduce the piecewise relation between γ and M as shown in Figure 4. To confirm the effect of polymer concentration, Φ = 0.13, 0.27, and 0.33 were

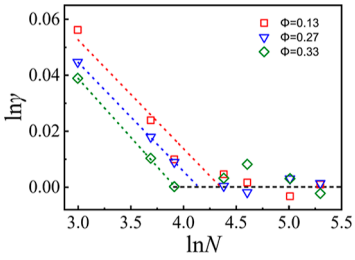

Figure 4. Effect of solution concentration on molecular weight dependence of surface tension in simulation. All tests were performed with $r_{cut} = 1.5\sigma$.

https://doi.org/10.1021/acs.jpcb.3c01719
J. Phys. Chem. B 2023, 127, 6743−6750

chosen. We can see M^* still appears earlier when solution concentration is increasing, as M^* = 80, 66, and 50 for Φ = 0.13, 0.27, and 0.33, respectively. On the other hand, $\alpha \approx -0.03$ is independent of the monomer volume fraction, which is consistent with the results observed in experiments. In order to verify the fact that M^* stands for the case of maximum of adsorption, we collect the adsorption amount in simulations directly. Adsorption amount Γ is defined as the number of monomer particles within 3σ of surface. The data of Γ when Φ = 0.13, 0.27, and 0.33 are shown in Figure 5. Clearly, Γ sharply

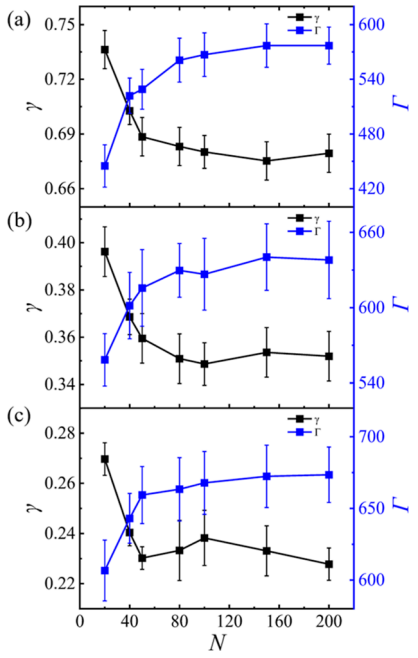

Figure 5. Adsorption amount Γ (blue line) and surface tension γ (black line) at different monomer concentrations, (a) Φ = 0.13, (b) Φ = 0.27, and (c) Φ = 0.33, with $r_{cut} = 1.5\sigma$.

increases and then levels off at any PEO concentration, characteristic of Langmuir adsorption. This further illustrates that the relation between γ and M in polymer solution should be resulted from adsorption of polymers. Furthermore, M^* is thus associated with the maximum of adsorption. According to the change in Γ with Φ, it is also confirmed that in the same solvent, higher monomer concentration will lead to higher saturation adsorbed amount. This can be attributed to the free energy difference between the surface and the bulk increases. Therefore, to reach equilibrium status, more monomers need to move to the surface. Additionally, this larger energy difference brings a larger driving force to polymers, the adsorption can thus reach saturation at a shorter chain length and M^* decreases.

The effect of solvent quality was explored by adjusting the cutoff distance in the simulation, as shown in Figure 6. Because this method may induce a pressure change, we checked pressure components along z-axis, $P_N(z)$, and $P_T(z)$, in the cases of $r_{cut} = 1.3\sigma$ and r_{cut} = 1.7, as shown in Figure S5. The results show that though there is slight change, the difference in $P_T(z)$ between the cases of $r_{cut} = 1.3\sigma$ and r_{cut} = 1.7 is only around 0.1 in all regions. The same is true for $P_N(z)$ in the bulk region. The significant change in $P_N(z)$ happens at the interface, which determines the value of surface tension. Therefore, we believe the change in pressure of system induced

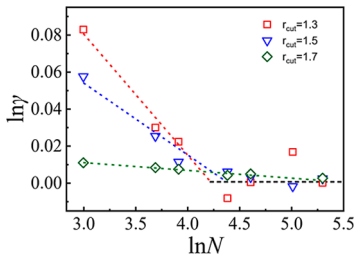

Figure 6. Effect of solvent on molecular weight dependence of surface tension in simulation. All tests were performed at Φ = 0.13.

by adjusting the solvent quality has little influence on our conclusion. In Figure 6, besides the piecewise relation between γ and M still persists, we still find a change value of α = −0.065, −0.039, and −0.005 for $r_{cut} = 1.3\sigma$, 1.5σ, and 1.7σ, respectively. However, this increase trend of α is not consistent with the experiment as shown in Figure 3, where α decreases as the solvent becomes better. We deem this is because the adsorption driving force depends on the difference between the energy of the surface and bulk. In our simulation, γ of the solvent is a constant because the interaction between solvent beads is not changed. By contrast, when the solvent is changed in the experiment section, γ of solvent also varies and influences the initial energy of the surface. For the complex effect of solvent, a concrete analysis according to specific situations is needed. On the another hand, M^* also still decreases with solvent becoming worse, as M^* = 67, 80, and 190 for $r_{cut} = 1.3\sigma$, 1.5σ, and 1.7σ, respectively. We also collect the adsorption amount in these cases and plot them in Figure 7. More chains were adsorbed to the surface in the worse solvent as shown in Figure 7, indicating that as r_{cut} increases, the solvent becomes better, and the interaction between polymer and solvent increases. As a result, polymer chains are effectively restricted to the bulk rather than adsorbed to the

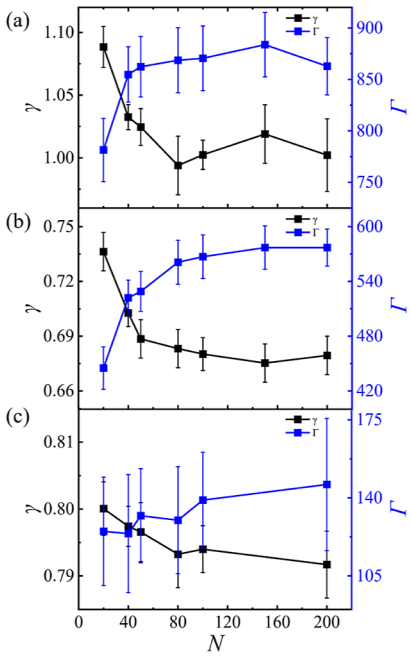

Figure 7. Adsorption amount of monomer (blue line) and γ (black line) in different solvents at Φ = 0.13, with (a) $r_{cut} = 1.3\sigma$, (b) $r_{cut} = 1.5\sigma$, and (c) $r_{cut} = 1.7\sigma$.

https://doi.org/10.1021/acs.jpcb.3c01719
J. Phys. Chem. B 2023, 127, 6743−6750

surface. In other words, the phase separation between the polymer and solvent is weakened, and a larger force is required to drive the chains from the bulk to the surface. That is why M^* increases as the solvent quality increases. Finally, we calculate the physical value of simulation system. The calculation details are in the Supporting Information section. For the absolute value of surface tension and adsorption amount between PEO solutions and simulation systems, the small deviation within the same order of magnitude is not important as the coarse-grained model is used. In addition, the mapping results show a similar trend of how an attractive surface influences the behavior of polymer chains in solution with the experiments, which further verifies the validity of the conclusions.

CONCLUSIONS

In conclusion, we have investigated the molecular weight M dependence of surface tension γ of PEO solutions. Generally, eq 1 works in a limited range of $M < M^*$, where M^* is the critical molecular weight. The physics behind M^* is the adsorption of polymer on air−liquid surface reaches the maximum at certain concentration. Different from that in polymer melts, adsorption plays a dominant role in the relation between γ and M in polymer solution. For an attractive surface, the adsorption driving force of polymer chains increases with M at a certain polymer concentration. The adsorption increases and γ goes down until $M = M^*$. When $M > M^*$, the adsorption and γ is independent of M. Furthermore, M^* decreases either as the solvent becomes worse or the monomer volume fraction increases. The exponent α of eq 1 is greatly affected by the surface tension of the solvent, which decreases as the solvent quality becomes worse in simulation. In addition, the solution concentration is not a prominent factor to change α.

ASSOCIATED CONTENT

Supporting Information

The Supporting Information is available free of charge at https://pubs.acs.org/doi/10.1021/acs.jpcb.3c01719.

Mean square radius of gyration of chains in simulation, schematic of the adsorption of PEO, data of surface tension of PEO in DME, effect of pressure in simulation, and result of mapping MD simulation to a physical system (PDF)

AUTHOR INFORMATION

Corresponding Authors

Jiajia Zhou − *South China Advanced Institute for Soft Matter Science and Technology, School of Emergent Soft Matter and Guangdong Provincial Key Laboratory of Functional and Intelligent Hybrid Materials and Devices, South China University of Technology, Guangzhou 510640, China;* orcid.org/0000-0002-2258-6757; Email: zhouj2@scut.edu.cn

Guangzhao Zhang − *Faculty of Materials Science and Engineering, South China University of Technology, Guangzhou 510640, China;* orcid.org/0000-0002-0219-3729; Email: msgzzhang@scut.edu.cn

Authors

Jianwei Zhang − *Faculty of Materials Science and Engineering, South China University of Technology, Guangzhou 510640, China*

Lu Qian − *Faculty of Materials Science and Engineering, South China University of Technology, Guangzhou 510640, China;* orcid.org/0000-0001-9038-3049

Complete contact information is available at: https://pubs.acs.org/10.1021/acs.jpcb.3c01719

Notes

The authors declare no competing financial interest.

ACKNOWLEDGMENTS

We thank the other members in the Ocean Engineering Materials Team from South China University of Technology for helpful discussions, assistance of experiments, and computing resources. This work was supported by the National Natural Science Foundation of China (NSFC) through the grant no. 21774004 (to J.Z.), the Recruitment Program of Guangdong (no. 2016ZT06C322), and the 111 Project (no. B18023).

REFERENCES

(1) Wu, S. *Polymer Interface and Adhesion*; Routledge: London, U.K., 2017.

(2) Chen, H.-X.; Zhang, E.-S.; Hong, M.; Liu, W.; Dai, X.-M.; Chen, Q.; Qiu, X.-P.; Ji, X.-L. Molecular Weight Dependence of Associative Behavior in Polyimide/DMF Solutions. *Chin. J. Polym. Sci.* **2020**, *38*, 629−637.

(3) Mardi, S.; Pea, M.; Notargiacomo, A.; Yaghoobi Nia, N.; Carlo, A. D.; Reale, A. The Molecular Weight Dependence of Thermoelectric Properties of Poly (3-Hexylthiophene). *Materials* **2020**, *13*, 1404.

(4) Ransom, T. C.; Roy, D.; Puskas, J. E.; Kaszas, G.; Roland, C. M. Molecular Weight Dependence of the Viscosity of Highly Entangled Polyisobutylene. *Macromolecules* **2019**, *52*, 5177−5182.

(5) Yu, K.; Hodges, C.; Biggs, S.; Cayre, O. J.; Harbottle, D. Polymer Molecular Weight Dependence on Lubricating Particle−Particle Interactions. *Ind. Eng. Chem. Res.* **2018**, *57*, 2131−2138.

(6) Wu, M.; Zhang, H.; Liu, H. Study of phase separation behavior of poly(N,N-diethylacrylamide) in aqueous solution prepared by RAFT polymerization. *Polym. Bull.* **2019**, *76*, 825−848.

(7) Legrand, D. G.; Gaines, G. L. The molecular weight dependence of polymer surface tension. *J. Colloid Interface Sci.* **1969**, *31*, 162−167.

(8) Sauer, B. B.; Dee, G. T. Surface Tensions of Molten Polymers as a Function of Molecular Weight and Temperature. *MRS Proc.* **1991**, *248*, 441−446.

(9) Dee, G. T.; Sauer, B. B. The molecular weight and temperature dependence of polymer surface tension: Comparison of experiment with interface gradient theory. *J. Colloid Interface Sci.* **1992**, *152*, 85−103.

(10) Sauer, B. B.; Dee, G. T. Molecular Weight Dependence of Surface Tension of Linear Perfluorinated Alkane Melts Including High Molecular Weight Poly(tetrafluoroethylenes). *Macromolecules* **1994**, *27*, 6112−6116.

(11) Legrand, D. G.; Gaines, G. L. Surface tension of homologous series of liquids. *J. Colloid Interface Sci.* **1973**, *42*, 181−184.

(12) Kamal, M. R.; Lai-Fook, R.; Demarquette, N. R. Interfacial tension in polymer melts. Part II: Effects of temperature and molecular weight on interfacial tension. *Polym. Eng. Sci.* **1994**, *34*, 1834−1839.

(13) Jo, W. H.; Lee, H. S.; Lee, S. C. Temperature and molecular weight dependence of interfacial tension between immiscible polymer pairs by the square gradient theory combined with the Flory-Orwoll-

Vrij equation-of-state theory. *J. Polym. Sci., Part B: Polym. Phys.* **1998**, *36*, 2683−2689.
(14) Dee, G. T.; Sauer, B. B. The surface tension of polymer liquids. *Adv. Phys.* **1998**, *47*, 161−205.
(15) De Gennes, P.-G. Tension superficielle des polymères fondus. *Acad. Sci., C. R. Ser. II* **1988**, *307*, 1841−1844.
(16) Aubouy, M.; Manghi, M.; Raphael, E. Interfacial properties of polymeric liquids. *Phys. Rev. Lett.* **2000**, *84*, 4858−4861.
(17) Kumar, S. K.; Jones, R. L. Comment on "Interfacial properties of polymeric liquids". *Phys. Rev. Lett.* **2001**, *87*, 179601.
(18) Ausserre, D. On the contribution of the chain ends to the surface tension of a polymer melt. *Eur. Phys. J. E* **2018**, *41*, 74.
(19) Aubouy, M.; Manghi, M.; Raphaël, E.; Aubouy, M.; Reply, R. Aubouy, Manghi, and Raphaël Reply: *Phys. Rev. Lett.* **2001**, *87*, 179602.
(20) Meddah, C.; Milchev, A.; Sabeur, S. A.; Skvortsov, A. M. Molecular weight effects on interfacial properties of linear and ring polymer melts: A molecular dynamics study. *J. Chem. Phys.* **2016**, *145*, 194902.
(21) Hilliard, J. E.; Cahn, J. W. On the nature of the interface between a solid metal and its melt. *Acta Metall.* **1958**, *6*, 772−774.
(22) Poser, C. I.; Sanchez, I. C. Surface tension theory of pure liquids and polymer melts. *J. Colloid Interface Sci.* **1979**, *69*, 539−548.
(23) Kumar, S. K.; Jones, R. L. Dominance of density variations in determining the molecular weight dependence of surface tensions of polymer melts. *Adv. Colloid Interface Sci.* **2001**, *94*, 33−38.
(24) Costa, N.; Li, P.; Xu, Y.; Liang, J.; Shivkumar, S. Effect of contact angle on the morphology of nanostructures produced by solution wetting of anodized aluminum oxide templates. *J. Nanopart. Res.* **2018**, *20*, 103.
(25) Zhang, J.; Lei, J.; Tian, W.; Zhang, G.; Floudas, G.; Zhou, J. Capillary Filling of Polymer Chains in Nanopores. *Macromolecules* **2023**, *56*, 2258−2267.
(26) Alazzam, A. Solution-based, flexible, and transparent patterned reduced graphene oxide electrodes for lab-on-chip applications. *Nanotechnology* **2019**, *31*, 075302.
(27) Washburn, E. W. The dynamics of capillary flow. *Phys. Rev.* **1921**, *17*, 273−283.
(28) Coppola, S.; Miccio, L.; Wang, Z.; Nasti, G.; Ferraro, V.; Maffettone, P. L.; Vespini, V.; Castaldo, R.; Gentile, G.; Ferraro, P. Instant in situ formation of a polymer film at the water−oil interface. *RSC Adv.* **2022**, *12*, 31215−31224.
(29) Li, Y.; Hu, K.; Han, X.; Yang, Q.; Xiong, Y.; Bai, Y.; Guo, X.; Cui, Y.; Yuan, C.; Ge, H.; Chen, Y. Phase Separation of Silicon-Containing Polymer/Polystyrene Blends in Spin-Coated Films. *Langmuir* **2016**, *32*, 3670−3678.
(30) Bianchi, M.; Limones Herrero, D.; Valle, F.; Greco, P.; Ingo, G.; Kaciulis, S.; Biscarini, F.; Cavallini, M. One-step substrate nanofabrication and patterning of nanoparticles by lithographically controlled etching. *Nanotechnology* **2011**, *22*, 355301.
(31) Gayrard, M.; Voronkoff, J.; Boissière, C.; Montero, D.; Rozes, L.; Cattoni, A.; Peron, J.; Faustini, M. Replacing Metals with Oxides in Metal-Assisted Chemical Etching Enables Direct Fabrication of Silicon Nanowires by Solution Processing. *Nano Lett.* **2021**, *21*, 2310−2317.
(32) Flory, P. J. *Principles of polymer chemistry*; Cornell university press: New York, 1953.
(33) Gaines, G. L. Surface tension of polymer solutions. IV. Three-component mixtures. *J. Polym. Sci.* **1972**, *10*, 1529−1535.
(34) Ueberreiter, K.; Morimoto, S.; Steulmann, R. Surface tension of polymer solutions. *Colloid Polym. Sci.* **1974**, *252*, 273−277.
(35) Bolten, D.; Türk, M. Experimental Study on the Surface Tension, Density, and Viscosity of Aqueous Poly(vinylpyrrolidone) Solutions. *J. Chem. Eng. Data* **2011**, *56*, 582−588.
(36) Gaines, G. L. Surface tension of polymer solutions. I. Solutions of poly(dimethylsiloxanes). *J. Phys. Chem.* **1969**, *73*, 3143−3150.
(37) Lipatov, Y. S.; Feinerman, A. E. The Concentration Dependence of Surface Tension of Polymer Solutions. *J. Adhes.* **2006**, *3*, 3−12.
(38) Tönsmann, M.; Ewald, D. T.; Scharfer, P.; Schabel, W. Surface tension of binary and ternary polymer solutions: Experimental data of poly(vinyl acetate), poly(vinyl alcohol) and polyethylene glycol solutions and mixing rule evaluation over the entire concentration range. *Surf. Interfaces* **2021**, *26*, 101352.
(39) Ober, R.; Paz, L.; Taupin, C.; Pincus, P.; Boileau, S. Study of the surface tension of polymer solutions: theory and experiments. Good solvent conditions. *Macromolecules* **1983**, *16*, 50−55.
(40) Poser, C. I.; Sanchez, I. C. Interfacial tension theory of low and high molecular weight liquid mixtures. *Macromolecules* **1981**, *14*, 361−370.
(41) Yang, H. E.; Bae, Y. C. Thermodynamic analysis of phase equilibrium and surface tension of ternary polymer solutions. *AlChE J.* **2019**, *65*, No. e16679.
(42) De Gennes, P. G. Polymer solutions near an interface. Adsorption and depletion layers. *Macromolecules* **1981**, *14*, 1637−1644.
(43) Aubouy, M.; Guiselin, O.; Raphaël, E. Scaling Description of Polymer Interfaces: Flat Layers. *Macromolecules* **1996**, *29*, 7261−7268.
(44) Gilanyi, T.; Varga, I.; Gilanyi, M.; Meszaros, R. Adsorption of poly(ethylene oxide) at the air/water interface: a dynamic and static surface tension study. *J. Colloid Interface Sci.* **2006**, *301*, 428−435.
(45) Kim, M. W.; Cao, B. H. Additional Reduction of Surface Tension of Aqueous Polyethylene Oxide (PEO) Solution at High Polymer Concentration. *Europhys. Lett.* **1993**, *24*, 229−234.
(46) Rennie, A. R.; Crawford, R. J.; Lee, E. M.; Thomas, R. K.; Crowley, T. L.; Roberts, S.; Qureshi, M. S.; Richards, R. W. Adsorption of poly(ethylene oxide) at the air-solution interface studied by neutron reflection. *Macromolecules* **1989**, *22*, 3466−3475.
(47) Schwuger, M. J. Mechanism of interaction between ionic surfactants and polyglycol ethers in water. *J. Colloid Interface Sci.* **1973**, *43*, 491−498.
(48) Siow, K. S.; Patterson, D. Surface thermodynamics of polymer solutions. *J. Phys. Chem.* **1973**, *77*, 356−365.
(49) Kim, M. W. Surface activity and property of polyethyleneoxide (PEO) in water. *Colloids Surf., A* **1997**, *128*, 145−154.
(50) Varga, I.; Keszthelyi, T.; Mészáros, R.; Hakkel, O.; Gilányi, T. Observation of a Liquid−Gas Phase Transition in Monolayers of Alkyltrimethylammonium Alkyl Sulfates Adsorbed at the Air/Water Interface. *J. Phys. Chem. B* **2005**, *109*, 872−878.
(51) Irving, J.; Kirkwood, J. G. The statistical mechanical theory of transport processes. IV. The equations of hydrodynamics. *J. Chem. Phys.* **1950**, *18*, 817−829.
(52) Allen, M. P.; Tildesley, D. J. *Computer Simulation of Liquids*; Oxford University Press: Oxford, U.K., 2017.
(53) Plimpton, S. Fast parallel algorithms for short-range molecular dynamics. *J. Comput. Phys.* **1995**, *117*, 1−19.
(54) Lu, J. R.; Su, T. J.; Thomas, R. K.; Penfold, J.; Richards, R. W. The determination of segment density profiles of polyethylene oxide layers adsorbed at the air-water interface. *Polymer* **1996**, *37*, 109−114.
(55) Noskov, B.; Akentiev, A.; Loglio, G.; Miller, R. Dynamic surface properties of solutions of poly (ethylene oxide) and polyethylene glycols. *J. Phys. Chem. B* **2000**, *104*, 7923−7931.
(56) Chen, C.-Y.; Even, M. A.; Wang, J.; Chen, Z. Sum frequency generation vibrational Spectroscopy studies on molecular conformation of liquid polymers poly (ethylene glycol) and poly (propylene glycol) at different interfaces. *Macromolecules* **2002**, *35*, 9130−9135.
(57) Mark, J. E. *Polymer Data Handbook*; Oxford University Press: Oxford, U. K., 2009.
(58) Eklund, T.; Britcher, L.; Bäckman, J.; Rosenholm, J. B. Thermogravimetric Analysis of γ-Aminopropyl-trimethoxysilane Adsorbed on Silica Support. *J. Therm. Anal. Calorim.* **1999**, *58*, 67−76.
(59) Jensen, G. V.; Shi, Q.; Deen, G. R.; Almdal, K.; Pedersen, J. S. Structures of PEP−PEO Block Copolymer Micelles: Effects of Changing Solvent and PEO Length and Comparison to a Thermodynamic Model. *Macromolecules* **2011**, *45*, 430−440.
(60) Luettmer-Strathmann, J. Lattice Model for Thermodiffusion in Polymer Solutions. *Int. J. Thermophys.* **2005**, *26*, 1693−1707.

https://doi.org/10.1021/acs.jpcb.3c01719
J. Phys. Chem. B 2023, 127, 6743−6750

(61) Zhao, Y.; You, L.-Y.; Lu, Z.-Y.; Sun, C.-C. Dissipative particle dynamics study on the multicompartment micelles self-assembled from the mixture of diblock copolymer poly(ethyl ethylene)-block-poly(ethylene oxide) and homopolymer poly(propylene oxide) in aqueous solution. *Polymer* **2009**, *50*, 5333−5340.
(62) Li, S.; Zhang, Y.; Liu, H.; Yu, C.; Zhou, Y.; Yan, D. Asymmetric Polymersomes from an Oil-in-Oil Emulsion: A Computer Simulation Study. *Langmuir* **2017**, *33*, 10084−10093.

https://doi.org/10.1021/acs.jpcb.3c01719
J. Phys. Chem. B 2023, 127, 6743−6750

Supporting Information

Molecular Weight Dependence of Surface Tension of Poly(ethylene oxide) Solution

Jianwei Zhang [1], Lu Qian [1], Jiajia Zhou [2,3,*], Guangzhao Zhang [1,*]

1. Faculty of Materials Science and Engineering, South China University of Technology, Guangzhou 510640, China
2. South China Advanced Institute for Soft Matter Science and Technology, School of Emergent Soft Matter, South China University of Technology, Guangzhou 510640, China
3. Guangdong Provincial Key Laboratory of Functional and Intelligent Hybrid Materials and Devices, South China University of Technology, Guangzhou 510640, China

1. Summary of previous works

Methods	Authors	Polymer	Scaling
Experiments	Legrand and Gaines	Poly(isobutylene) Poly(dimethylsiloxane)	$\gamma \sim M^{-2/3}$
Experiments	Dee and Sauer	Poly(ethylene glycol) Poly(propylene glycol) Polyethylene	$\gamma \sim M^{-2/3}$ & $\gamma \sim M^{-1}$
Experiments	Siow and Patterson	Poly(dimethylsiloxane)	$\gamma \sim M^{-2/3}$ & $\gamma \sim M^{-1}$
Experiments	Jo and Lee	Polystyrene Poly(methyl methacrylate)	$\gamma \sim M^{-2/3}$ & $\gamma \sim M^{-1}$
Scaling Functional Theory	de Gennes	/	$\gamma \sim M^{-1/2}$
Scaling Functional Theory	Aubouy	/	$\Delta\gamma \propto \ln(M/M*)/M^{1/2}$
Self-consistent Field	Wu	/	$\gamma \sim M^{-1}$
Standard Mean-field	Kumar	/	$\gamma \sim M^{-1}$

Table S1. Comparison the research on the scaling relation between surface tension γ and molecular weight M of polymer melt.

2. Mean square radius of gyration of chains in simulation

The mean square radius of gyration R_g of polymer chains is calculated in a box with periodic boundary conditions in all directions, and other parameters are all same with that in the Simulation Details section. We collect R_g of polymer chains in equilibrium with

$$R_g^2 = \sum_i [(x_i - x_{cm})^2 + (y_i - y_{cm})^2 + (z_i - z_{cm})^2] \quad \text{(S1)}$$

where the subscript i stands for the ith bead and cm stands for the center of mass of chains. The results are shown in Fig. S1.

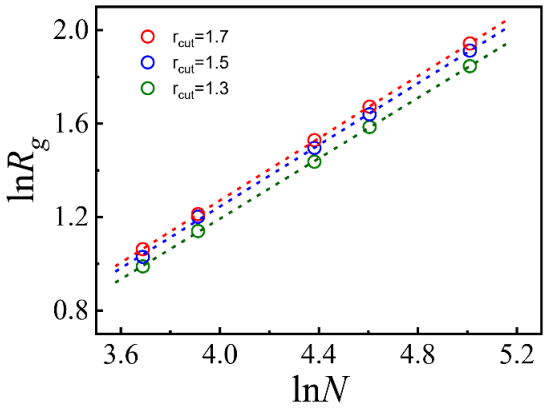

Figure S1. The scaling relation between the mean square radius of gyration R_g and the degree of polymerization N at different r_{cut} values.

3. Finite-size effect

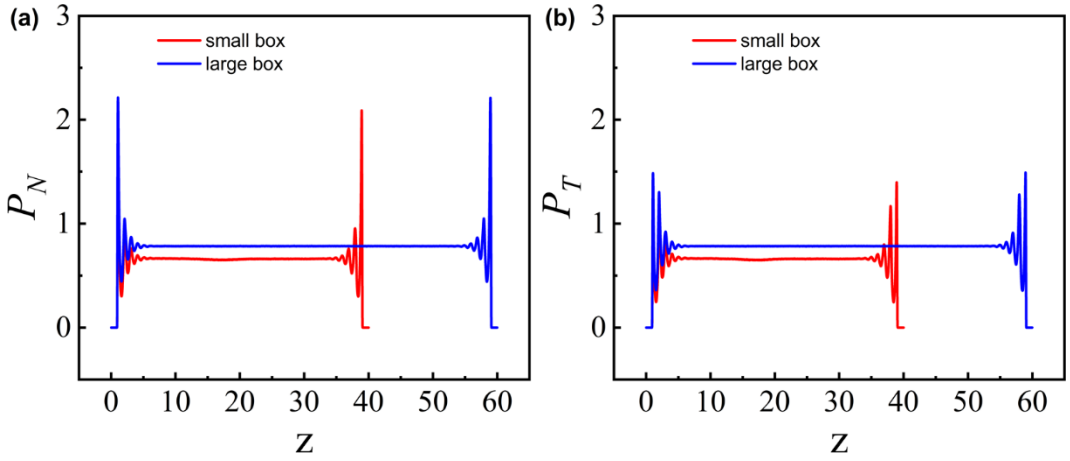

Figure S2. Comparison of pressure components distribution along z-axis (a) $P_N(\mathrm{z})$ and (b) $P_T(\mathrm{z})$ of system of $N = 200$, when box size is $L_x = L_y = 25\,\sigma$, $L_z = 40\,\sigma$ (small box) and $L_x = L_y = 40\,\sigma$, $L_z = 60\,\sigma$ (large box).

4. M* and Adsorption of PEO

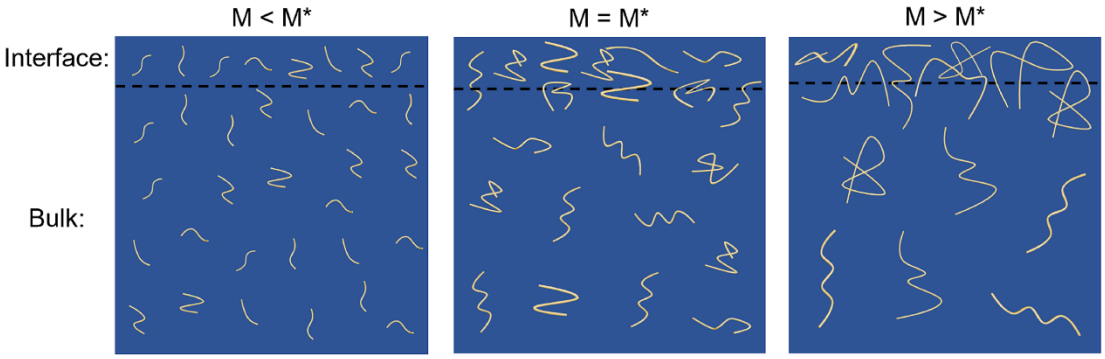

Figure S3. The schematic of the adsorption of PEO when $M < M^*$, $M = M^*$, and $M > M^*$.

5. Surface Tension

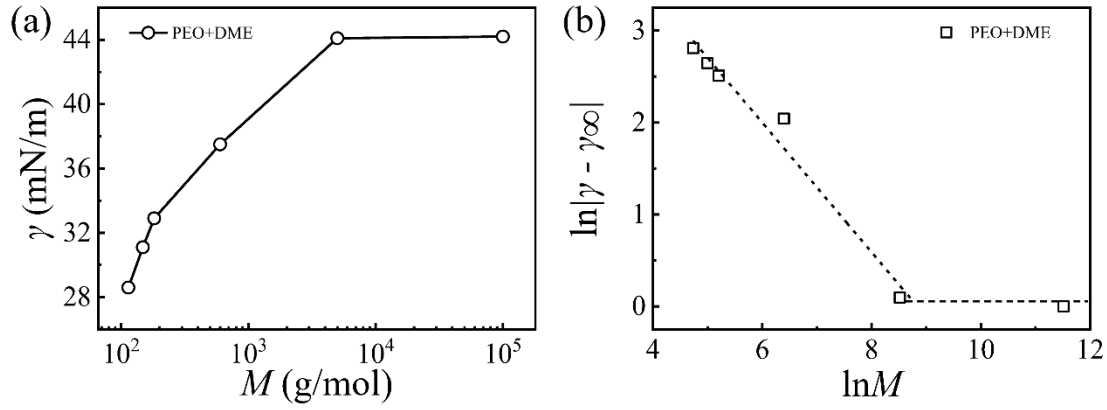

Figure S4. The relation between surface tension γ and molecular weight M of PEO in DME at 20 ℃. The data were collected from Polymer Data Handbook.[1]

6. Pressure

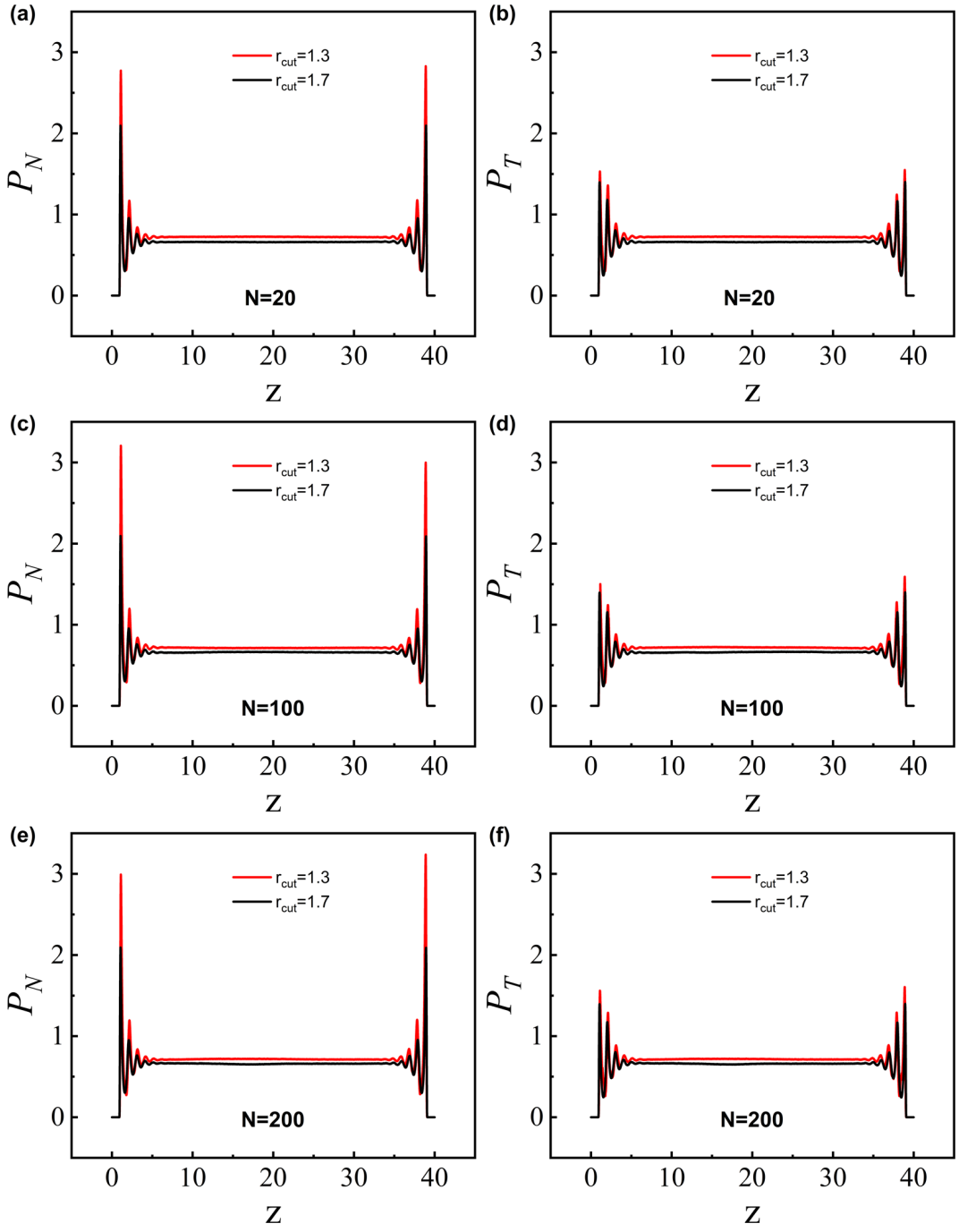

Figure S5. Comparison of pressure components distribution along z-axis between when $r_{cut} = 1.3\,\sigma$ and $r_{cut} = 1.7\,\sigma$ for (a) $P_N(\mathrm{z})$ and (b) $P_T(\mathrm{z})$ in the case of $N = 20$, (c) $P_N(\mathrm{z})$ and (d) $P_T(\mathrm{z})$ in the case of $N = 100$, and (e) $P_N(\mathrm{z})$ and (f) $P_T(\mathrm{z})$ in the case of $N = 200$ in simulation.

7. Mapping simulation to real system

We follow the common coarse-graining method obtain the physical value of simulation system.[2] To adopt reduced units in our simulation, we set the unit of energy is $\varepsilon = k_B T$ with $T = 298\ K$ and a bead represents a molecule with volume equals to $72\ \text{Å}^3$, about 1.2 EO groups. As system density ρ equals to 0.72, the unit of length in real system can be given as $\sigma = \sqrt[3]{0.72 \times 72}\ \text{Å}^3 = 3.7\ \text{Å}$, and the unit of mass $m = \frac{1.2\times44}{6.023\times10^{-23}} = 8.8 \times 10^{-23} g$. Time unit then can be given as $\tau = \sqrt{\mathrm{m}\sigma^2/\varepsilon} = 1.7\ ps$.

When value of surface tension in simulation γ_{MD} equals to 1, value of surface tension in real system can be given as $\gamma_{real} = \frac{\gamma_{MD} k_B T}{\sigma^3} = 30\ mN/m$. When value of adsorption amount in simulation Γ_{MD} equals to 500, the value of adsorption amount in real system can be given as $\Gamma_{real} = \frac{\Gamma_{MD}\mathrm{m}}{\sigma^2} = 0.52\ mg/m^2$.

References

(1) Mark, J. E. *Polymer data handbook*. Oxford university press: Oxford, U. K., 2009.

(2) Groot, R. D.; Rabone, K. Mesoscopic simulation of cell membrane damage, morphology change and rupture by nonionic surfactants. *Biophys. J.* **2001,** *81*, 725-736.